

On the use of $Ti_{50}Be_{40}Zr_{10}$ as a spring material

F. G. YOST

Sandia National Laboratories, Albuquerque, NM 87185, USA*

A useful figure-of-merit for spring material candidates is derived and computed for a select group of iron and titanium alloys. Two commercially available amorphous alloys are shown to have considerably more attractive figures-of-merit than do several crystalline alloys. Since springs left in a stressed condition must resist stress relaxation, tests of this type were performed on an amorphous titanium alloy. The results indicate that relaxation kinetics depend upon initial heat treatment but are independent of initial applied stress. This behaviour is shown to be consistent with hyperbolic flow in the limit of low stress. A simple least-squares analysis of the relaxation kinetics yields an activation energy of 67 kJ mol^{-1} . When used for springs, this alloy should be heat treated.

1. Introduction

Applications of metallic glass are increasing rapidly as more investigators become intrigued by their interesting properties. Magnetic components which rely upon the high permeability and saturation magnetization of commercially available metallic glass alloys have received careful attention [1–4]. For reasons of handling ease, economy and improved strength, amorphous brazing alloys are enjoying an expanding market [5]. Higher crystallization temperatures, strength and corrosion resistance promise many obvious and unforeseen applications of this interesting class of materials. Their practical use as spring materials apparently has not been recognized in the literature. Material used in a spring component must be fabricable, have adequate fatigue strength and acceptable corrosion resistance. In addition, since springs are frequently left in a stressed condition, they must resist low-temperature stress relaxation.

An elastic analysis is reported here that provides a useful figure-of-merit for spring material candidates called spring force effectiveness. This figure-of-merit was computed for a few select iron- and titanium-based alloys, often used for springs, and is compared to that computed for two com-

mercially available amorphous alloys. It will be seen that amorphous alloys are, indeed, a very attractive material for spring components. Also reported are coiled ribbon stress relaxation tests performed at three initial stress levels on as-received Metglas 2204[†] ribbons. Similar testing was carried out at the intermediate stress level on similar ribbons previously annealed at 523 K for 7.2 ksec under zero stress. The stress relaxation tests were carried out at five temperatures so that an Arrhenius analysis of the data will allow prediction of room-temperature behaviour of spring components. The results are presented and discussed in the light of previous stress relaxation tests of this type.

2. Experimental procedure

The stress relaxation test discussed by Luborsky *et al.* [6] and Graham *et al.* [7] has been used in these experiments; however, two test procedures were followed. Specimens in Group A were 0.05 mm thick by 1.00 mm wide Metglas 2204 ribbon in the as-received condition. Specimens in Group B were these same ribbons heat treated under zero stress at 523 K for 7.2 ksec prior to the stress relaxation tests. Aluminium blocks, 3.73 cm

*A U.S. Department of Energy Facility.

[†]This $Ti_{50}Be_{40}Zr_{10}$ alloy is produced by Allied Chemical, PO Box 1021R, Morristown, NJ 07960, USA.

long by 1.27 cm wide by 0.318 cm thick, containing holes bored at 0.476, 0.635 and 0.953 cm diameter were used to confine the ribbons during stress relaxation. The ribbons were cut to fit the circumference of the holes when coiled and inserted. The stress relaxation heat treatments were carried out at five temperatures ranging from 423 to 523 K (in 25 K increments) in stirred oil baths capable of maintaining ± 1 K.

To determine how repeatable the experiment was, a separate specimen was used for each point in the Group A set of data. For the Group B data, each of the five specimens was re-used to obtain subsequent data points at longer stress relaxation times. After each anneal, the specimen was removed from the aluminium block and its radius of curvature was measured with an optical comparator which had a resolution of 0.25 mm. The data were reduced by calculating the ratio of the bending moment, $M(t)$, after anneal time, t , to that at $t = 0$, $M(0)$

$$\frac{M(t)}{M(0)} = \frac{\int_0^{d/2} \sigma(z, t) z dz}{\int_0^{d/2} \sigma(z, 0) z dz}, \quad (1)$$

where z is a co-ordinate perpendicular to and beginning at the neutral axis, d is the ribbon thickness and $\sigma(z, t)$ is the local stress. Later, this relationship will prove useful when certain flow models, $\sigma(z, t)$, are compared with the experimental data. The ratio, given in Equation 1 and designated R , is also given by

$$R = \frac{1 - R_h/R_t}{1 - R_h/R_s}, \quad (2)$$

where R_h is the hole radius, R_s is the unconstrained radius at $t = 0$ and R_t is the unconstrained radius after anneal time t . While being stored on a spool, this material assumes a permanent set resulting in a finite R_s -value. Estimates of error in R may be calculated using the resolution 0.25 mm and allowing R_t to take on the values $R_t = \pm 0.25$ mm. Consequently this error becomes larger as R_t and R decrease.

3. Elastic analysis

Consider a flat spring element, having thickness d and width w , bent into a contour having radius of curvature, $C(s)$, where s is the arc length along the neutral axis. Then the elastic energy, U , in the spring is given by [8]

$$U = \oint \frac{M^2(s) ds}{2EI}, \quad (3)$$

where $M(s)$ is the bending moment, E is the elastic modulus and

$$I = wd^3/12 \quad (4)$$

is the moment of inertia. Substituting the definition of the bending moment

$$M(s) = \frac{EI}{d/2 + C(s)} \cong \frac{EI}{C(s)}, \quad (5)$$

and the above expression for I into Equation 3 yields

$$U = \frac{EWd^3}{24} \oint \frac{ds}{C^2(s)}. \quad (6)$$

The maximum strain in this spring element is

$$\epsilon_m = \frac{\sigma_m}{E} = \frac{d/2}{d/2 + C_{\min}} \cong \frac{d}{2C_{\min}}, \quad (7)$$

where C_{\min} is the smallest bending radius encountered along s . Consequently, to avoid plastic deformation and a permanent set, the maximum allowable thickness would be

$$d_m = \frac{2\sigma_m C_{\min}}{E}, \quad (8)$$

where σ_m is the elastic-plastic proportional limit which, for amorphous alloys, is approximately equal to the yield stress. Substituting Equation 8 into Equation 6 gives an expression for the upper bound of the stored elastic energy

$$U = \frac{\sigma_m^3}{E^2} \frac{WC_{\min}^2}{3} \oint \frac{ds}{C^2(s)}. \quad (9)$$

The quantity

$$F = \frac{\sigma_m^3}{E^2} \quad (10)$$

has been called spring force effectiveness [9] and is the figure-of-merit referred to previously. The spring force effectiveness is a combination of material properties, whereas the remainder of Equation 9 is geometric in origin. It would be desirable to make F large so that the force per unit of volume exerted by the spring would be large. This quantity has been calculated for several spring steels and strong titanium alloys as well as for commercially available iron-based and titanium-based amorphous alloys; the results are shown in Table I. Notice that there is a decided difference between the iron-based crystalline alloys and the iron-boron amorphous alloy as well as between

TABLE I Spring force effectiveness for selected ferrous and titanium alloys

Alloy	Condition	Spring force effectiveness
15-5	H-900	0.037
4130	Quenched and tempered	0.082
440C	Hardness and stress relieved	0.159
52100	Quenched and tempered	0.908
Metglas 2605 (Fe ₈₀ B ₂₀)	As-cast	1.649
Ti 5-2.5	Quenched	0.086
Ti 6-4	Aged	0.125
Ti 7-4	Aged and extruded	0.139
Ti 6-6-2	Extruded and aged	0.165
Metglas 2204 (Ti ₅₀ Be ₄₀ Zr ₁₀)	As-cast	1.030

the titanium-based crystalline alloys and the titanium–beryllium–zirconium amorphous alloy. The spring force effectiveness for the glass alloy is approximately an order of magnitude larger than that for the crystalline alloys. Yield strengths and elastic moduli data for these calculations were taken from [10] and details regarding alloy chemistry and preparation can be found therein. Measurements have shown that the velocity of sound [11] in Metglas 2204 changes approximately 4% upon annealing at 523 K for 7.2 ksec under zero stress; therefore, its elastic modulus changes approximately 8% since negligible changes in density are expected. These structural modifications are not sufficient to make the spring force effectiveness of the crystalline alloys comparable with that of amorphous alloys.

4. Stress relaxation results and discussion

As mentioned in Section 2, separate as-received specimens were used for each data point in Group A to obtain some indication of the repeatability of the stress relaxation behaviour. As a result, the data are expected to be more scattered than that in Group B where fewer specimens were used. Group A data are plotted in Figs 1, 2 and 3 corresponding to the three increasing initial outer fibre stress levels. Each figure includes data from five stress relaxation temperatures and, except for the two highest temperatures, the data fall on remarkably smooth curves, suggesting a high degree of experimental repeatability. At all temperatures and stresses a rapid initial drop is observed in the stress relaxation parameter, R . Then a more gradual stress relaxation tendency is observed. The severity of the initial drop appears to increase in both extent and rate with increasing temperature.

This behaviour was also apparent in the data of Graham *et al.* [7] which was discussed and analysed by Ast and Krenitsky [12]. At any given temperature, data from Figs 1, 2 and 3 superimpose indicating that R is independent of initial outer fibre stress. This observation suggests that stress in the coiled ribbon should be of the form

$$\sigma(z, t) = \sigma_0 S(z, t), \quad (11)$$

where $S(z, t)$ is independent of σ_0 , the initial outer fibre stress. If this relationship for $\sigma(z, t)$ is substituted into Equation 1 it can be seen that $R(t)$ would be independent of σ_0 . This apparent independence would not have been predicted from the analysis of Ast and Krenitsky [12] since in either of their derived relationships for stress

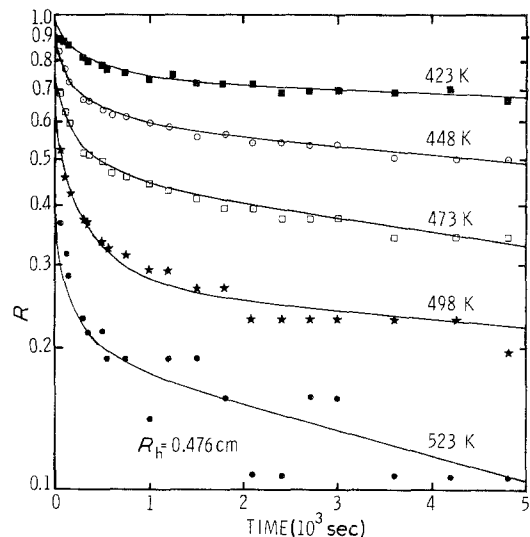


Figure 1 Stress relaxation of as-received Metglas 2204 ribbon (coil radius of 0.476 cm) against anneal time at five temperatures.

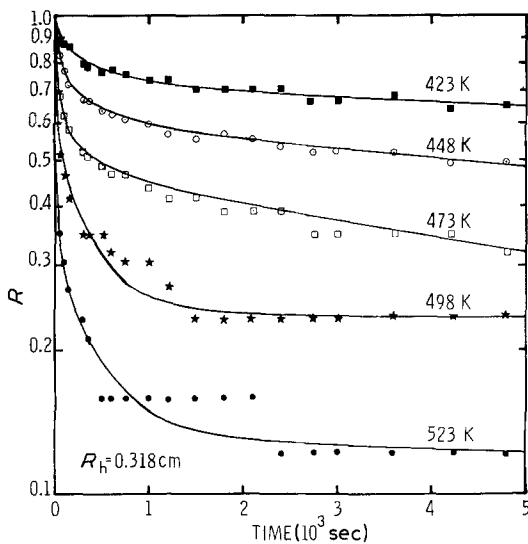


Figure 2 Stress relaxation of as-received Metglas 2204 ribbon (coil radius of 0.318 cm) against anneal time at five temperatures.

relaxation kinetics, in the form $M(t)/M(0) = R(t)$, there is a more complex dependence on σ_0 . However the hyperbolic flow model analysed by Ast and Krenitsky [12] can be put into the form of Equation 11. When

$$\sigma(z, 0)v^* \ll 2kT,$$

expansion to first order yields

$$\sigma(z, t) = \frac{2z\sigma_0}{d} \cdot \exp(-t/\tau), \quad (12)$$

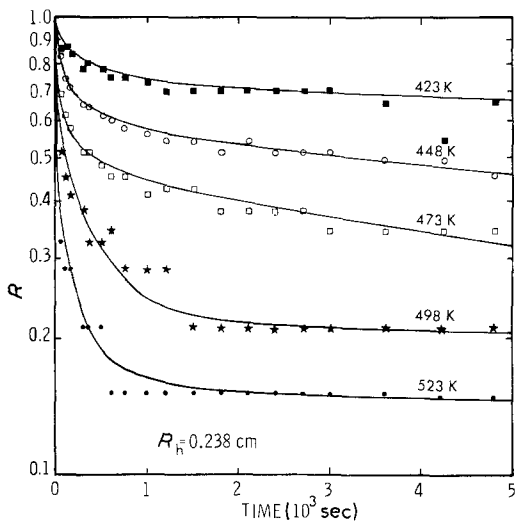


Figure 3 Stress relaxation of as-received Metglas 2204 ribbon (coil radius of 0.238 cm) against anneal time at five temperatures.

where [12]

$$\tau = \frac{kT \exp(\Delta H/kT)}{2E\dot{\epsilon}_0 v^*}, \quad (13)$$

where $\dot{\epsilon}_0$ is a pre-exponential factor, v^* is an activation volume and ΔH is the activation energy for transient creep, which is the form of Equation 11. It is not apparent how one can eliminate the dependence of $M(t)/M(0)$ on σ_0 using the power-law creep model which is Equation 8 of Ast and Krenitsky [12].

The rapid initial drop and gradual relaxation behaviour observed in the Group A data and that of Graham *et al.* [7] are highly suggestive of two or more flow processes. This is especially significant when it is realized that the data are plotted on a logarithmic co-ordinate. Using numerical fits of their two flow models Ast and Krenitsky [12] concluded that one process, namely hyperbolic flow, is capable of describing the stress relaxation kinetics of as-received Metglas 2826B. As will be shown, the heat treatment of the Group B specimens appears to simplify the stress relaxation kinetics by suppressing one or more flow processes.

Group B data are obtained from specimens which were first annealed at 523 K for 7.2 msec under zero stress, then stress relaxed. These data are plotted against annealing time in Fig. 4. The data obtained at 423 K are not plotted since relaxation at this temperature was so slow that crowded plotting symbols made the graph difficult to read. Quite an obvious change in relaxation behaviour has taken place. The non-steady state behaviour, characterized by a rapid initial drop, is no longer apparent. Consequently, while the rapid relaxation behaviour of as-received material might prevent its use as a spring material, a low-temperature heat treatment, prior to use, restores its potential.

The kinetics exhibited by the Group B specimens appear to be similar to the gradual second-stage kinetics of the Group A specimens. These more gradual kinetics have been called isoconfigurational or steady-state homogeneous flow [13, 14]. The almost linear behaviour suggests a simple exponential decay of the ratio of bending moments, R . By combining Equations 1, 2 and 12 one finds

$$\ln R = -\frac{t}{\tau} \quad (14)$$

so a least-squares analysis of the data was performed in the natural logarithmic domain to ob-

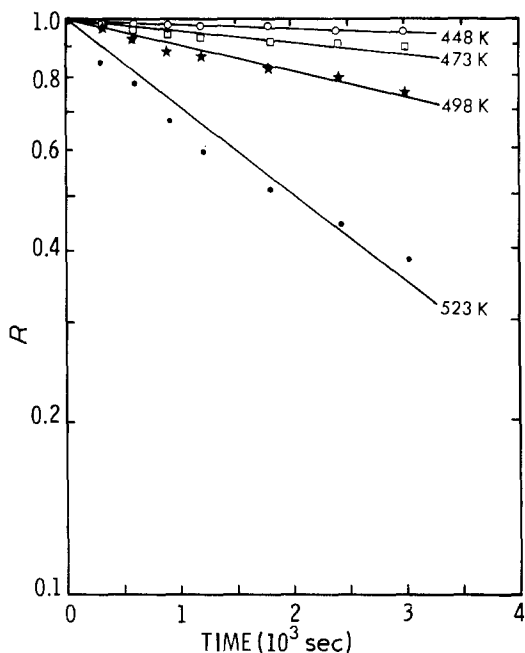


Figure 4 Stress relaxation of heat treated Metglas 2204 ribbon (coil radius of 0.318 cm) against anneal time at four temperatures.

tain the straight lines in Fig. 4. The slopes of these lines are, according to Equation 14, equal to $-1/\tau$. The relaxation times, τ , were then divided by the test temperature in degrees Kelvin and plotted against reciprocal degrees Kelvin as suggested by Equation 13. The calculated relaxation times show a slight curvature, but of opposite sign to that expected for glasses [15]. The curvature may be due to temper embrittlement [16] or may simply be due to statistical scatter in the data. More work is necessary to resolve this question. A standard Arrhenius analysis yielded an activation energy of 67 kJ mol^{-1} which is much less than that calculated by Ast and Krenitsky [12] for Metglas 2826B. At the risk of oversimplification, it is suggested that this isoconfigurational flow can be described by Equation 12. In this way the stress relaxation parameter, R , is independent of σ_0 and decreases linearly in the natural logarithmic domain. To ensure the inequality used to obtain Equation 12 the volume of a flow unit, v^* , must be of the order of 10 \AA^3 . By way of contrast, Taub [14] quotes 48 \AA^3 for $\text{Pd}_{82}\text{Si}_{18}$ and Ast and Krenitsky [12] calculated 400 \AA^3 for Metglas 2826B.

5. Conclusion

An elastic analysis has shown that spring force effectiveness is a useful figure-of-merit for selecting spring materials. Two commercially available

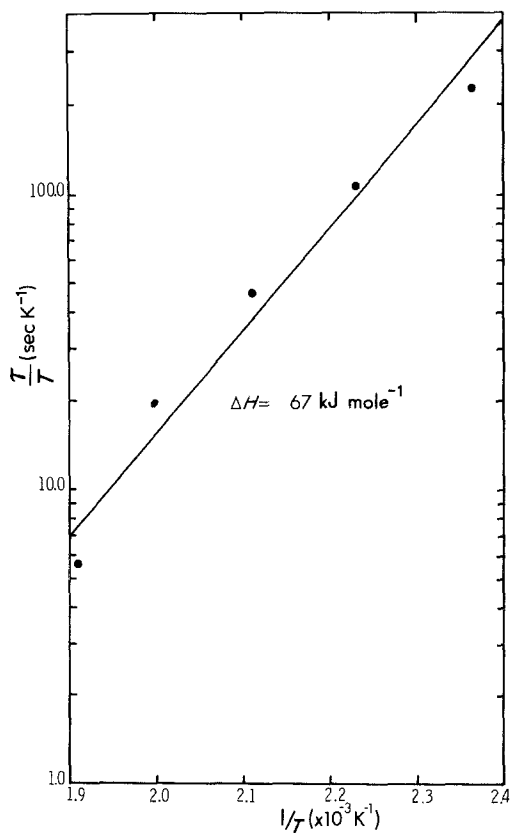


Figure 5 Relaxation time τ divided by absolute temperature against reciprocal degrees Kelvin. An activation energy of 67 kJ mol^{-1} was calculated.

amorphous alloys were shown to have an extremely large spring force effectiveness relative to that of typical crystalline alloys, making them excellent candidates for spring applications. As-received Metglas 2204 appears to stress relax in two stages. Stress relaxation kinetics for this alloy are independent of initial applied stress. Annealed material relaxes in simple exponential fashion with an activation energy of 67 kJ mol^{-1} and an activation volume of approximately 10 \AA^3 . If used as a spring material, this alloy must be annealed to avoid rapid initial relaxation.

Acknowledgements

The author wishes to thank K. S. Varga and J. H. Gieske for their technical assistance. This work was supported by the US Department of Energy (DOE) under Contract No. DE-ACO4-76-DP00789.

References

1. F. E. LUBORSKY, *IEEE Trans. Magn.* **14** (1978) 1008.
2. F. E. LUBORSKY, J. J. BECKER, P. G. FRISCH-

- MANN and L. A. JOHNSON, *J. Appl. Phys.* **49** (1978) 1769.
3. F. E. LUBORSKY, P. G. FRISCHMANN and L. A. JOHNSON, *J. Magn. Mater.* **8** (1978) 318.
 4. L. I. MENDELSON, E. A. NESBITT and G. R. BRETT, *IEEE Trans. Magn.* **12** (1976) 924.
 5. N. DeCRISTOFARO and C. HENSCHER, *Welding J.* **57** (1978) 33.
 6. F. E. LUBORSKY, J. J. BECKER and R. O. McCARY, *IEEE Trans. Magn.* **11** (1975) 1644.
 7. C. D. GRAHAM, JR, T. EGAMI, R. S. WILLIAMS and Y. TAKEI, "Magnetism and Magnetic Materials", edited by J. J. Becker, G. H. Lander and J. J. Rhyne, (American Institute of Physics, New York, 1976) p. 218.
 8. S. TIMOSHENKO and D. H. YOUNG "Elements of Strength Materials" 5th edn. (D. VanNostrand Company, Inc, New York (1978) p. 220.
 9. M. S. WALMER, "First Symposium on Rolamite", (University of New Mexico Press, Albuquerque, 1969) p. 65.
 10. "Aerospace Structural Metals Handbook", Mechanical Properties Data Center, Battelle Columbus Laboratories (1981).
 11. J. H. GIESKE, unpublished work 1980.
 12. D. G. AST and D. J. KRENITSKY, *J. Mater. Sci.* **14** (1979) 287.
 13. A. S. ARGON, *Acta Metall.* **27** (1979) 47.
 14. A. I. TAUB, *ibid.* **28** (1980) 633.
 15. D. R. UHLMANN and R. W. HOPPER, "Metallic Glasses", edited by J. J. Gilman and H. J. Leamy, (American Society for Metals, Metals Park, 1978) p. 128.
 16. L. A. DAVIS, *ibid.* p. 190.

Received 6 January and accepted 9 April 1981.